Published OnlineFirst June 21, 2017; DOI: 10.1158/1535-7163.MCT-16-0881

Companion Diagnostics and Cancer Biomarkers

Molecular Cancer Therapeutics

Modulation of Plasma Metabolite Biomarkers of the MAPK Pathway with MEK Inhibitor RO4987655: Pharmacodynamic and Predictive Potential in Metastatic Melanoma

Joo Ern Ang[1,2], Akos Pal[1], Yasmin J. Asad[1], Alan T. Henley[1], Melanie Valenti[1], Gary Box[1], Alexis de haven Brandon[1], Victoria L. Revell[3], Debra J. Skene[3], Miro Venturi[4], Ruediger Rueger[5], Valerie Meresse[6], Suzanne A. Eccles[1], Johann S. de Bono[1,2], Stanley B. Kaye[1,2], Paul Workman[1], Udai Banerji[1,2], and Florence I. Raynaud[1,2]

Abstract

MAPK pathway activation is frequently observed in human malignancies, including melanoma, and is associated with sensitivity to MEK inhibition and changes in cellular metabolism. Using quantitative mass spectrometry–based metabolomics, we identified in preclinical models 21 plasma metabolites including amino acids, propionylcarnitine, phosphatidylcholines, and sphingomyelins that were significantly altered in two B-RAF–mutant melanoma xenografts and that were reversed following a single dose of the potent and selective MEK inhibitor RO4987655. Treatment of non–tumor-bearing animals and mice bearing the PTEN-null U87MG human glioblastoma xenograft elicited plasma changes only in amino acids and propionylcarnitine. In patients with advanced melanoma treated with RO4987655, on-treatment changes of amino acids were observed in patients with disease progression and not in responders. In contrast, changes in phosphatidylcholines and sphingomyelins were observed in responders. Furthermore, pretreatment levels of seven lipids identified in the preclinical screen were statistically significantly able to predict objective responses to RO4987655. The RO4987655 treatment–related changes were greater than baseline physiological variability in nontreated individuals. This study provides evidence of a translational exo-metabolomic plasma readout predictive of clinical efficacy together with pharmacodynamic utility following treatment with a signal transduction inhibitor. *Mol Cancer Ther; 16(10); 2315–23. ©2017 AACR.*

Introduction

The MAPK cascade (the Ras/Raf/MEK/ERK pathway) is a receptor tyrosine kinase–mediated signaling pathway that regulates cell proliferation, cell-cycle progression, and cell migration (1). The frequent constitutive activation of RAS and RAF proteins has been well-established in human malignancies (2). Mutations in the genes encoding members of the RAF protein family have been documented in 20% of cancers and 66% of melanomas (2–6). This pathway has been targeted at various loci, and inhibitors of B-RAF, MEK, and ERK have been developed (7). A number of MEK inhibitors such as trametinib and RO4987655 have shown activity in *B-RAF*– and *N-RAS*–mutant metastatic melanoma (8, 9). In these studies, currently utilized biomarkers including *B-RAF* and *N-RAS* mutations are not completely predictive, with responses observed in patients not harboring these mutations (10).

We have previously shown that plasma metabolite markers of PI3K inhibition identified in mouse models were confirmed in a phase I clinical trial of pictilisib (GDC-0941). The changes observed are consistent with the insulin resistance phenotype developing upon treatment with PI3K inhibitors (11). In the present study, we evaluated whether circulating metabolites also represent attractive biomarkers to assess the sensitivity and response to MEK inhibitors. We implemented an exploratory screen for plasma metabolites exhibiting changes associated with MAPK modulation using a validated quantitative LC/MS-MS–based metabolomic analysis (Biocrates Absolute IDQ p180 kit). We first compared plasma samples from female athymic mice bearing xenografts of *B-RAF*–mutant WM266.4 and A375 human melanoma with their non–tumor-bearing age-matched littermates. We next evaluated the effect of a single dose of RO4987655 on the plasma metabolite concentrations in treated animals compared with vehicle controls. We identified a metabolomics

[1]Cancer Research UK Cancer Therapeutics Unit, The Institute of Cancer Research, London, United Kingdom. [2]Drug Development Unit, The Royal Marsden NHS Foundation Trust, Sutton, United Kingdom. [3]Faculty of Health and Medical Sciences, University of Surrey, Guildford, United Kingdom. [4]F. Hoffmann-LaRoche Ltd., Diagnostics Division, DIA Biomarker Group, Basel, Switzerland. [5]Roche Pharmaceutical Research and Early Development, Translational Medicine Oncology, Roche Innovation Center Penzberg, Penzberg, Germany. [6]Roche Pharmaceutical Research and Early Development, Translational Medicine Oncology, Roche Innovation Center Basel, Basel, Switzerland.

J.E. Ang and A. Pal contributed equally to this article and are joint first authors.

Note: Supplementary data for this article are available at Molecular Cancer Therapeutics Online (http://mct.aacrjournals.org/).

Corresponding Author: F.I. Raynaud, The Institute of Cancer Research, Division of Cancer Therapeutics, London SW7 3RP, United Kingdom. Phone: 442087224212; Fax: 442087224126; E-mail: Florence.Raynaud@icr.ac.uk

doi: 10.1158/1535-7163.MCT-16-0881

©2017 American Association for Cancer Research.

Downloaded from mct.aacrjournals.org on November 30, 2020. © 2017 American Association for Cancer Research.

Published OnlineFirst June 21, 2017; DOI: 10.1158/1535-7163.MCT-16-0881

signature consistent with MAPK activation and reversed by treatment with the MEK inhibitor. We then evaluated this signature in U87MG glioma xenografts which are driven by loss of PTEN (and thus an activated PI3 kinase pathway) following treatment with the MEK inhibitor RO4987655.

We tested the hypothesis that the levels of these plasma metabolites may reflect the degree of MAPK pathway activation (e.g., via *B-RAF* mutation) and that these novel biomarkers may be predictive of clinical outcome in addition to having pharmacodynamic utility following MEK inhibitor therapy. We tested our preclinical metabolomic signature in 35 evaluable patients with relapsed, metastatic melanoma treated with RO4987655, at the MTD in a nonrandomized open-label phase I clinical trial (12). We examined the effect of treatment on metabolite concentrations and the relationship between pretreatment baseline levels of the metabolite biomarker candidates and objective response determined by RECIST criteria (12) in 35 patients. Time-of-day variation can affect significantly the plasma metabolome (13, 14). To assess the potential confounding impact of this factor on the candidate biomarkers, we studied the degree of variation of these metabolites in 35 subjects with advanced melanoma and in 12 healthy male volunteers over 24 hours.

We show that the metabolomics signature identified in the preclinical setting in the sensitive melanoma xenografts is recapitulated in patients and that baseline levels of seven candidate biomarkers are prognostic of clinical response.

Materials and Methods

In the exploratory preclinical screening studies, we compared plasma from female athymic mice 6 to 8 weeks of age inoculated subcutaneously with human WM266.4 or A375 (*B-RAF*–mutant) melanoma cells with samples from their age-matched non–tumor-bearing controls. Next, tumor-bearing and non–tumor-bearing animals were randomized to receive the MTD of RO4987655 (6 mg/kg) or cremaphor/methanol/water (1/1/3) vehicle. RO4987655 was provided by Chugai. We selected plasma metabolites that were different in tumor-bearing mice compared with non–tumor-bearing controls and changes that were reversed by addition of a single dose of the MEK inhibitor in both xenograft models.

A metabolic signature identified from these studies was then tested in the $PTEN^{(-/-)}$-null U87MG human glioblastoma xenograft. The signature was also tested in the phase I clinical study with RO4987655 in patients with advanced metastatic melanoma. Finally, we applied the MEK signature to patients with advanced solid tumors in a phase I clinical study of the PI3K inhibitor pictilisib (clinicaltrials.gov identifier: NCT00876122; refs. 15, 16).

Preclinical human tumor xenograft studies

All animal experiments were conducted in accordance with local and UK National Cancer Research Institute guidelines (17). WM266.4 melanoma cells (ATCC lot #3272826, 02/13/2003), A375 (ATCC lot #61573377 07/07/2015 2015), and U87MG glioblastoma cells (ATCC lot unavailable; obtained 07/10/2008) were profiled and authenticated in house (2015). Cell lines were analyzed by short tandem repeat (STR) profiling. Polymorphic STR loci were amplified using a PCR primer set. The PCR product (each locus was labeled with a different fluorophore) was analyzed simultaneously with size standards by using an automated fluorescent detection technique. The number of repeats at 7 to 10 different loci defines the STR profile and was cross-referenced with online databases to confirm authenticity. All cell lines showed 100% match and were mycoplasma negative.

For pharmacodynamic and metabolomic experiments, 2 million cells were injected subcutaneously bilaterally into the flanks of female NCr athymic mice 6 to 8 weeks of age, bred in-house. During the experiment, food pellets (Certified Rodent Diet 5002, Labdiet) and water were available *ad libitum*. Dosing of the animals was undertaken synchronously under sterile conditions in the same experiment when tumors were well-established and approximately 8 to 10 mm in diameter. A single dose of 6 mg/kg RO4987655 was administered p.o. in cremaphor/methanol/water. Control animals received an equivalent volume of vehicle. Blood and tumor samples were collected at the following times after drug administration: 2, 4, 8, and 24 hours (WM266.4); 2, 4, and 8 hours (A375), and 2, 8, and24 hours (U87MG). Five mice were used for each time point per treatment. For therapy studies, 3 million cells were injected subcutaneously into right flanks, and mice (10/group) were dosed p.o. with 6 mg/kg RO4987655 or with vehicle for 12 (WM266.4) or 16 days (A375).

In pharmacodynamics, metabolomics, and therapy studies, blood samples were collected (using sodium heparin as anticoagulant) and tumors were snap frozen. The blood samples were centrifuged at 13,000 rpm for 2 minutes, and the plasma transferred onto dry ice; the entire process from collection to storage in dry ice took less than 5 minutes per sample. Plasma and tumor samples were stored at −80°C until further analysis.

Meso Scale Discovery assay

Meso Scale Discovery (MSD) 96-well multispot assays were carried out according to the manufacturer's protocol with minor modifications. Briefly, ERK1/2 (duplex) plate was blocked (MSD blocking solution, as recommended by the manufacturer, plus 0.1% BSA) for 1 hour at room temperature with shaking and then washed 4 times. Ten microgram of total protein of tumor homogenates was added in duplicate wells and incubated overnight at 4°C. Plates were washed as previously; then 25 μL of detection antibody was added and incubated at room temperature for 2 hours with shaking. Plates were washed 4 times, 150 μL of read buffer was added, and the plates were analyzed on a MESO QuickPlex SQ 120. The two additional spots in each well coated with BSA were used to correct for the background and for any effects of the lysis buffer. Data shown are the mean values of left and right tumors of the pharmacodynamic experiments (five tumors per time point per treatment).

Phase I expansion trial of RO4987655

Plasma samples for metabolomic analysis were obtained from 35 patients with advanced metastatic melanoma treated as part of an expansion phase I study with RO4987655 (10). Patients received 8.5 mg RO4987655 twice daily for 28-day cycles, and metabolomic samples were collected before dose, and 8 and 24 hours after dose on day 1 and cycle 2 day 1 (day 29). Plasma was separated from blood (using sodium heparin as anticoagulant) following centrifugation at 1,500 *g* for 15 minutes at 4°C; it was then stored at −80°C until further analysis. All aspects of the study were conducted in accordance with the Declaration of Helsinki and the International Conference on Harmonization Good Clinical Practice Guidelines. Written informed consent was obtained from all participants. The details of the phase I study, the

Downloaded from mct.aacrjournals.org on November 30, 2020. © 2017 American Association for Cancer Research.

Published OnlineFirst June 21, 2017; DOI: 10.1158/1535-7163.MCT-16-0881

metabolomics sample collection, and analysis of pictilisib responses have been described previously (15, 16).

Plasma metabolomics analysis

We carried out targeted, quantitative metabolomic analysis by electrospray ionization tandem MS using the AbsoluteIDQ p180 Kit (Biocrates Life Sciences AG). Samples were anonymized and randomized, and analyses were carried out on a Waters Acquity H-class UPLC coupled to Xevo TQ-S triple-quadrupole MS/MS System (Waters Corporation). Quantification of the metabolites of the biological sample was achieved by reference to appropriate internal standards. The method follows the United States Food and Drug Administration Guidelines "Guidance for Industry – Bioanalytical Method Validation (May 2001)," providing proof of reproducibility within a given error range.

Data analysis

The analytical process to derive metabolite concentrations was performed using MassLynx (Waters corporation) and the MetIDQ software package (Biocrates Life Sciences) Multivariate analysis was performed using SIMCA v.14.1 software (MKS Umetrics AB) to determine metabolite features that were differentially expressed between defined groups of mice: (1) WM266.4 tumor–bearing mice versus non–tumor-bearing animals; (2) non–tumor-bearing mice treated with vehicle or 6 mg/kg RO498766; and (3) RO-treated (6 mg/kg) versus vehicle-treated mice bearing WM266.4 tumors. The same analysis was carried out in mice bearing A375 tumors. Metabolites responsible for differences were identified using orthogonal partial least square-discriminant analysis (OPLS-DA; ref. 18) with a threshold of variable importance in the projection value >0.5 and cross-validation by permutation analysis carried out. To pass the exploratory preclinical screen and establish the signature, a metabolite was required to be affected consistently across tumor-bearing mice versus controls and to show reverse changes in xenograft-bearing mice treated with a single dose of the MEK inhibitor. For the relevant plasma metabolites at each time point, the changes relative to control concentration (pretreatment or vehicle) were used to generate heatmaps. We tested the metabolomics signature identified in melanoma mice with an additional cohort bearing PTEN-null U87MG human glioblastoma xenografts following treatment with a single dose of the MEK inhibitor.

In the clinical studies with the MEK inhibitor and the PI3K inhibitor, we focused on the metabolites that had been identified in the preclinical studies. Changes relative to pretreatment baseline levels were calculated for each patient across all time points for each metabolite. In the study with the MEK inhibitor, the separation between the response categories of disease progression and objective RECIST response was assessed using the receiver operator characteristic (ROC) curve. The statistical significance of the differences was determined using Mann–Whitney, Kruskal–Wallis, and Dunn's multiple comparison tests (Graphpad Prism v6), and values < 0.05 were considered statistically significant. The Venn diagram was generated on http://bioinformatics.psb.ugent.be/webtools/Venn/ website. Clustered heatmap diagram was constructed using MetaboAnalyst 3.0 (19).

Results

Preclinical models

RO4987655 inhibits ERK phosphorylation and tumor growth in human melanoma xenografts. Following a single dose of 6 mg/kg RO4987655 to female athymic mice bearing s.c. human B-RAF–mutant melanoma xenograft WM266.4 or A375, a complete inhibition of ERK phosphorylation was observed in tumors at 2, 6, and 8 hours after treatment in both models (Fig. 1A and B). This target modulation resulted in significant tumor growth inhibition following daily treatment with RO4987655 at 6 mg/kg with T/C of 16% and 3.5%, respectively (Fig. 1C). This schedule was well tolerated with no body weight loss.

The metabolomics workflow is summarized in Fig. 2A.

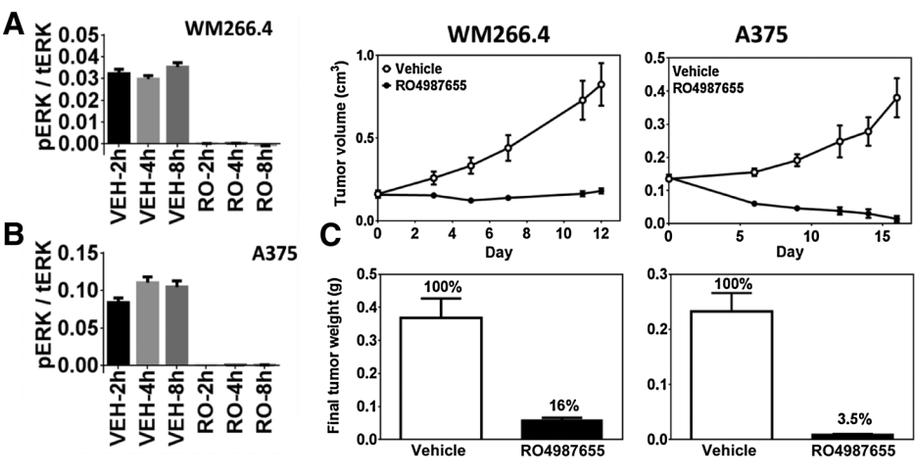

Figure 1.

A and **B**, Inhibition of ERK phosphorylation by RO4987655 in WM266.4 and A375 human melanoma xenografts. Ratio of phosphorylated (pERK) and total ERK (tERK) demonstrates total inhibition of phosphorylation of ERK in both melanoma models after RO4987655 (RO) administration compared with vehicle control (VEH), measured by MSD. Values are mean ± SEM of left and right tumors. **C,** Tumor growth inhibition following daily treatment with RO4987655 in WM266.4 and A375 human melanoma xenografts. Target modulation resulted in significant growth inhibition following daily treatment with RO4987655 at 6 mg/kg with T/C of 16% and 3.5% in WM266.4 and A375 tumor–bearing mice, respectively. Values are mean ± SEM.

Downloaded from mct.aacrjournals.org on November 30, 2020. © 2017 American Association for Cancer Research.

Published OnlineFirst June 21, 2017; DOI: 10.1158/1535-7163.MCT-16-0881

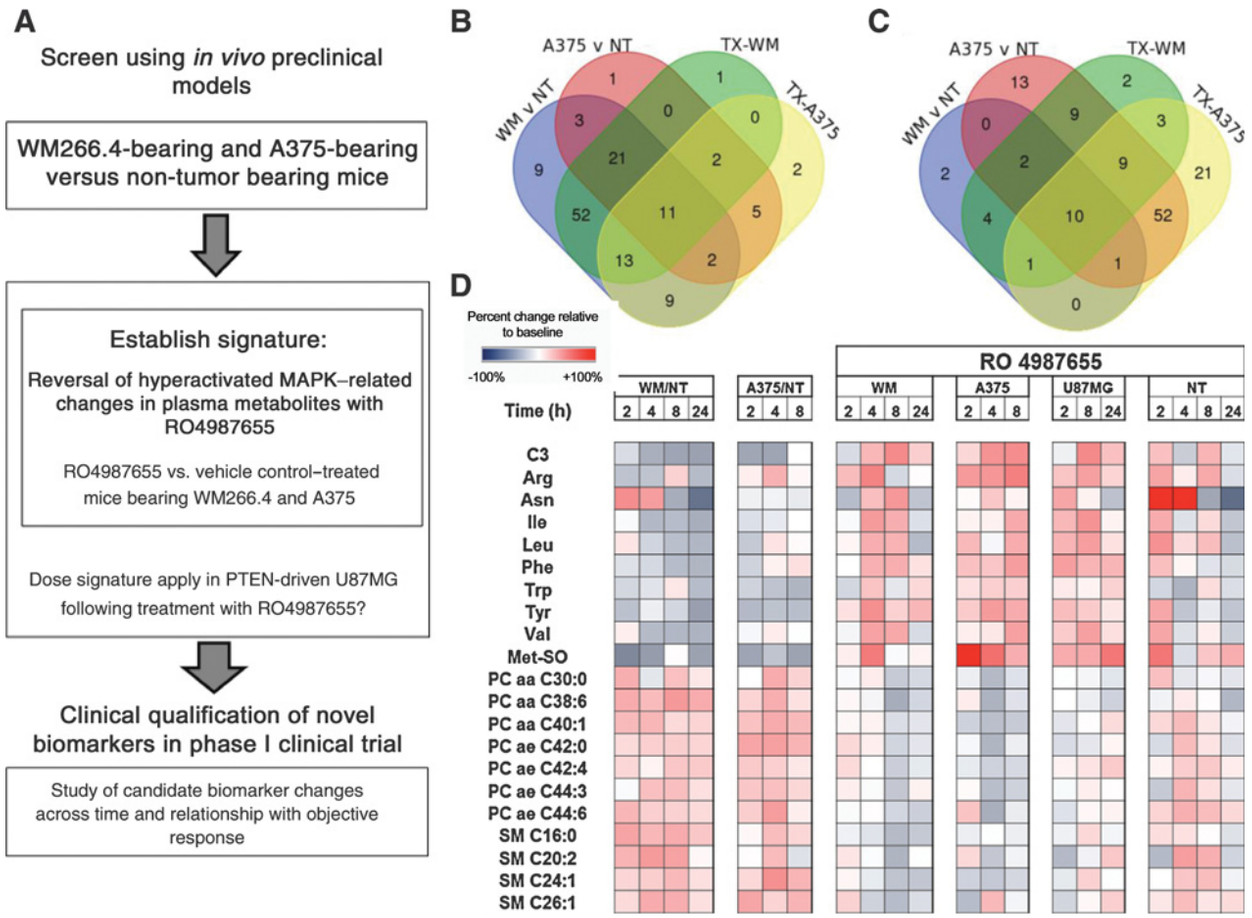

Figure 2.

Metabolomic analysis of plasma from tumor-bearing mice or control mice treated with RO4987655. **A,** Experimental workflow. **B** and **C,** Venn diagrams showing the overlap in plasma metabolites between preclinical animal models: (**A**) metabolites increased in WM266.4 and A375 tumor–bearing mice compared with non–tumor-bearing age-matched controls and decreased in the tumor-bearing mice treated with RO4987655 compared with vehicle; or *vice versa* (**B**). **D,** Heatmap of differences between MAPK-hyperactivated tumor-bearing mice compared with age-matched non–tumor-bearing littermates (change relative to control) and changes across 24 hours in candidate plasma metabolite biomarkers following treatment with RO4987655 (relative to vehicle control) in tumor-bearing and non–tumor-bearing mice. (aa, acyl-acyl; ae, acyl-alkyl; Cx:y, where x is the number of carbons in the fatty acid side chain; y is the number of double bonds in the fatty acid side chain; PC, phosphatidylcholine; SM, sphingomyelin.)

Identification of the metabolomic signature. We compared plasma samples from mice bearing WM266.4 and A375 melanomas with their non–tumor-bearing age-matched littermates. OPLS-DA revealed 11 metabolites which were increased in these MAPK-driven tumors and decreased following RO4987655 treatment plus 10 metabolites which were decreased in the plasma of tumor-bearing mice and increased following treatment (summarized in Fig. 2B and C). Hence, a total of 21 metabolites including propionylcarnitine, arginine, asparagine, isoleucine, leucine, phenylalanine, tryptophan, tyrosine, valine, methylsulfoxide, 7 phosphatidylcholines (PC aa C30:0, PC aa 36:6, PC aa 40:1, PC ae 42:0, PC ae 44:3, and PC ae 44:6), and 4 sphingomyelins (SM 16:0, SM 20:2, SM C24:1, SM C26:1) were different in plasma of animals bearing *B-RAF*–mutant melanomas compared with controls and inversely affected by treatment with the MEK inhibitor. (Fig. 2D). Overall, propionylcarnitine and the amino acids were decreased in the plasma of tumor-bearing animals compared with controls and increased by treatment. In contrast, lipids were increased in plasma of tumor-bearing mice and decreased with treatment (Fig. 2D). In tumor-bearing mice, the metabolic effects were most pronounced at 4 and 8 hours and were different from those observed in non–tumor-bearing mice (Fig 2D). In the *PTEN*$^{(-/-)}$-null human glioblastoma xenograft (U87MG), which is not MAPK-dependent, a single dose of the MEK inhibitor had different effects on the plasma metabolites identified in melanoma models (Fig. 2D, fifth column) with only amino acids and propionylcarnitine increased following treatment with the MEK inhibitor. Reversed changes of lipid levels following RO4987655 treatment were observed only in melanoma xenograft models.

The metabolic effects following RO4987655 are different in clinical responders and patients with disease progression. We examined the relationship between all 182 metabolites and objective responses determined by RECIST criteria (12) in 35 evaluable patients treated with 8.5 mg/kg (i.e., the MTD) of RO4987655. The OPLS-DA model revealed a high degree of separation between

Downloaded from mct.aacrjournals.org on November 30, 2020. © 2017 American Association for Cancer Research.

Published OnlineFirst June 21, 2017; DOI: 10.1158/1535-7163.MCT-16-0881

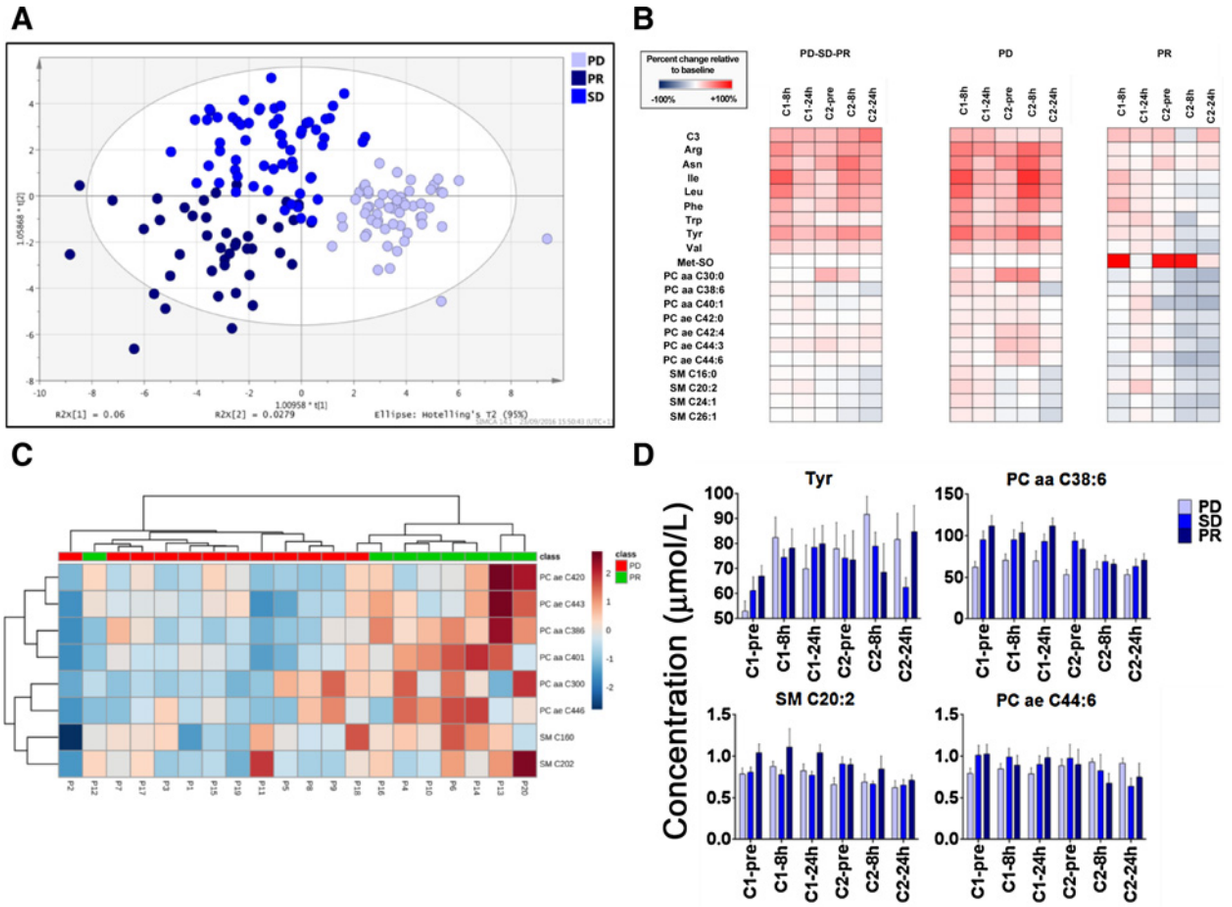

Figure 3.

Metabolomic profiling of RO4987655 in a phase I clinical trial. **A,** OPLS-DA according to response to RO4987655 in patient plasma metabolomic profiles across all time course of treatment (cycle 1 and cycle 2). A total of 182 metabolites were measured. **B,** Heatmap illustrating the changes relative to baseline treatment in 21 candidate metabolite biomarkers. Data are presented from left to right in all patients (PD-SD-PR column), in patients with progressive disease (PD column), in partial responders (PR column) on cycle 1 8h, cycle 1 24h, cycle 2 predose, cycle 2 8h, and cycle 2 24h. **C,** Heatmap of unsupervised clustering according to the pretreatment concentrations of 20 metabolites identified as predictors of response (MetaboAnalyst 3.0, Pareto scaling, Distance Measure: Euclidean; Clustering Algorithm: Ward). **D,** Concentrations of representative plasma metabolites in patients with metastatic melanoma at baseline and following treatment with RO4987655. Values are mean ± SEM in patients who achieved an objective response ($n = 8$; PR) or experienced disease progression ($n = 12$; PD).

the response categories of disease progression and objective RECIST response (Fig. 3A). The most significant effects were observed on propionylcarnitine and amino acids that showed an increase at all time points. The sphingomyelins and one phosphatidylcholine (PC aa C38:6) showed an overall decrease at 24 hours, but this was not statistically significant (Table 1, Fig. 3B, PD-PR-SD column). In addition, the metabolic alterations were significantly different between patients with disease progression and those who achieved an objective response (Fig. 3B, PD and PR columns). Overall, progressors showed a significant increase in amino acids relative to predose levels, whereas responders showed no significant increase in these amino acids up to cycle 2 at 24 hours. In addition, a significant decrease in 7 phospholipids was observed from cycle 2, which was not observed in patients who progressed. The metabolite changes observed in responsive patients were consistent with the effects observed in mice bearing the sensitive WM266.4 and A375 melanoma xenografts, and the effects in nonresponsive patients were in line with the effects in non–tumor-bearing mice or the U87MG xenograft model (Figs. 2C and 3B; Table 2). In addition, the effect of the PI3K inhibitor pictilisib on the MEK signature also showed an increase in the amino acids but no decrease in phospholipids, which is comparable with that observed in patients with progressive disease (PD) following RO4987655 administration. The effect on amino acids following pictilisib was not observed below 80 mg (suggesting that it is genuinely associated with PI3K inhibition and not disease progression; Supplementary Fig. S1).

Baseline levels of seven plasma metabolites predict clinical response to RO4987655. We examined the relationship between pretreatment baseline levels of the metabolite biomarker candidates and objective response determined by RECIST criteria (12) in 35 evaluable patients. Of 21 biomarker candidates, 7 plasma

Downloaded from mct.aacrjournals.org on November 30, 2020. © 2017 American Association for Cancer Research.

Published OnlineFirst June 21, 2017; DOI: 10.1158/1535-7163.MCT-16-0881

Table 1. Evaluation of the significance of the changes in metabolite levels compared with predose levels following treatment with the MEK inhibitor RO4987655

		Dunn's multiple comparison test									
	Kruskal–Wallis	C1-8h		C1-24h		C2-pre		C2-8h		C2-24h	
	P value	Mean	Adj. *P* value	Mean	Adj. *P* value	Mean	Adj. *P* value	Mean	Adj. *P* value	Mean	Adj. *P* value
Metabolites											
C3	**0.0016**	**28.46**	**0.0099**	**34.47**	**0.0004**	**24.83**	**0.0089**	24.8	0.1847	**43.53**	**0.0378**
Arg	<**0.0001**	**42.23**	<**0.0001**	**26.88**	**0.0036**	**24.54**	**0.0035**	**35.75**	**0.0024**	**35.27**	**0.0001**
Asn	<**0.0001**	**34.09**	<**0.0001**	**20.31**	**0.0008**	**28.25**	<**0.0001**	**47.25**	<**0.0001**	**35.67**	<**0.0001**
Ile	<**0.0001**	**59.14**	<**0.0001**	**31.88**	**0.0001**	15	0.3326	**47.95**	**0.0003**	**34.13**	**0.0021**
Leu	<**0.0001**	**47.26**	<**0.0001**	**26.16**	<**0.0001**	**14.79**	**0.0101**	**36.7**	**0.0001**	**26.67**	**0.0002**
Phe	<**0.0001**	**28.74**	<**0.0001**	**13.47**	**0.0198**	**19.79**	**0.0051**	**27.75**	**0.0027**	**25.93**	**0.0022**
Trp	**0.0371**	22.57	0.1073	15.94	0.1526	5.333	>0.9999	−0.55	>0.9999	3.733	>0.9999
Tyr	**0.0003**	**36.4**	**0.0004**	**27.56**	**0.0036**	**28.92**	**0.0216**	**35.5**	**0.0049**	**33.6**	**0.0015**
Val	**0.0004**	**16.49**	<**0.0001**	**13.41**	**0.0012**	8.375	0.0847	**11.9**	**0.0417**	**11.07**	**0.0206**
Met-SO	**0.0046**	**117.8**	**0.0348**	110.2	0.7205	355.7	0.4795	**162.8**	**0.0286**	**209.9**	**0.0034**
PC aa C30:0	0.2272	0.6286	>0.9999	2.156	>0.9999	25.17	0.4472	10.55	>0.9999	−1	>0.9999
PC aa C38:6	**0.0005**	4.286	>0.9999	4.844	>0.9999	−4.417	0.3513	−**9.1**	**0.0409**	−**16.67**	**0.0068**
PC aa C40:1	0.2189	3.8	>0.9999	6.75	>0.9999	−0.9167	>0.9999	−5.9	0.7959	−0.5333	>0.9999
PC ae C42:0	0.626	2.514	>0.9999	5.094	>0.9999	3.083	>0.9999	−3.45	>0.9999	1.467	>0.9999
PC ae C42:4	0.6558	0	>0.9999	2.531	>0.9999	9.417	>0.9999	−5	0.416	6.267	>0.9999
PC ae C44:3	0.7112	4.771	>0.9999	10.78	>0.9999	15.17	>0.9999	3.9	>0.9999	9.533	>0.9999
PC ae C44:6	0.6457	−0.8286	>0.9999	−1.594	>0.9999	6.542	>0.9999	−4.2	0.9183	0.1333	>0.9999
SM C16:0	**0.0019**	1.686	>0.9999	2.719	>0.9999	−1.292	0.297	−**11.85**	**0.006**	−**11.6**	**0.0093**
SM C20:2	**0.0317**	3.886	>0.9999	6.781	>0.9999	−1.25	0.8285	−**10.2**	**0.0484**	−9.867	0.0728
SM C24:1	0.1213	1	>0.9999	3.344	>0.9999	0.875	>0.9999	−10.1	0.1824	−8.667	0.2434
SM C26:1	**0.0096**	−1.057	>0.9999	2.688	>0.9999	0.375	>0.9999	−**13.55**	**0.0303**	−13	0.0591

NOTE: Statistical tests carried out are Kruskal–Wallis test for all time points and Dunn's multiple comparison tests for individual time points (*P* values <0.05 are bold). Mean values are percentage increase or decrease relative to time 0.

metabolites were significantly different between patients who responded and those who progressed (P values < 0.05), and all 7 metabolites exhibited an estimated area under the receiver operating characteristic curve of $\geq$0.75 (Table 3). The plasma levels of all these lipid metabolites were higher in patients who subsequently achieved an objective response to RO4987655. (Fig. 3B). In contrast, a poor separation between the metabolic profiles of patients harboring *B-RAF*–mutant and *B-RAF* wild-type melanomas was observed with only three metabolites correlating with *B-RAF* mutational status. The lack of a significant difference in these plasma metabolites between the two groups is summarized in Table 3.

A heatmap of an unsupervised analysis of the pretreatment levels of selected lipids (based on preclinical signature, Fig. 3C) shows clustering of 7 of 8 patients with partial response and 11 of 12 patients with PD (Fig. 3C).

Collectively, these results suggest hitherto-unknown biological pathways involving the panel of metabolite biomarkers being implicated in mechanisms underlying vulnerability of melanoma cells to MEK inhibition. A summary of the levels of four representative metabolites throughout the course of treatment is presented in Fig. 3D.

Changes in the metabolite biomarkers following RO4987655 exceed time-of-day variations. Time-of-day variation can affect significantly on the plasma metabolome (13, 14). To assess the potential confounding impact of this factor on the candidate biomarkers, we studied the degree of variation of these metabolites in an additional study (Supplementary Table S1). One study examined the variability of these metabolites in 35 subjects with advanced melanoma and the second evaluated time-of-day variation over a 24-hour period using the same clinical sampling schedule in 12 healthy male volunteers. Reassuringly, 90% of RO4987655-related changes (19 of 21) of the metabolite biomarkers were greater than the variability observed in these physiologic/time-of-day studies.

Discussion

This study provides evidence of plasma metabolites as biomarkers predictive of objective response to a molecularly targeted anticancer drug with good discrimination. The prior identification of biomarker candidates in molecularly characterized preclinical tumor screens where control animals were included significantly increases confidence that these metabolites represent genuine exo-metabolomic changes associated with MAPK pathway modulation.

We demonstrated that basal levels of 21 metabolites including amino acids, glycerophosphocholines, and sphingomyelins were differentially affected in clinical responders and progressors following treatment with RO4987655. In patients with PD, we observed an increase in amino acids and no decrease in lipids. This significant increase in amino acids was also observed following treatment with the PI3K inhibitor pictilisib where no therapeutic benefit was observed in all but one patient (15, 16). In patients responding to the MEK inhibitor, the amino acids and lipids were decreased. In addition, basal levels of seven metabolites (glycerophosphocholines and sphingomyelins) were significantly able to predict response with higher levels in responders. In contrast to the metabolite biomarker changes, the median decrease in ERK phosphorylation in tumors was higher in patients with a *B-RAF* mutation than those without, but there was no evidence of a significant difference in pERK inhibition between different response outcome groups (12). A previous study showed that reduction of p-ERK was correlated with response to the B-RAF inhibitor vemurafenib (20); however, there is published evidence that this is not the case for MEK inhibitors (12). In addition, the

Downloaded from mct.aacrjournals.org on November 30, 2020. © 2017 American Association for Cancer Research.

Published OnlineFirst June 21, 2017; DOI: 10.1158/1535-7163.MCT-16-0881

Table 2. Statistical analysis of the effect of treatment with RO4987655 on metabolites identified preclinically in patient with PD and partial response (PR)

	PD										PR									
					Dunn's multiple comparison test										Dunn's multiple comparison test					
	Kruskal–Wallis P	C1-8h		C1-24h		C2-pre		C2-8h		C2-24h	Kruskal–Wallis P	C1-8h		C1-24h		C2-pre		C2-8h		C2-24h	
			Adj. P		Adj. P		Adj. P		Adj. P				Adj. P		Adj. P		Adj. P		Adj. P		Adj. P
Metabolites	value	Mean	value	Mean	value	Mean	value	Mean	value	Mean	value	Mean	value	Mean	value	Mean	value	Mean	value	Mean	value
C3	0.2294	29.42	0.1505	27.58	0.1348	14	0.3537	11.86	>0.9999	14.17	0.6901	0.6324	43.13	>0.9999	30	0.4572	29	>0.9999	23	>0.9999	78.2	>0.9999
Arg	**0.0043**	50.33	**0.0022**	41.08	**0.0499**	35.38	0.1106	57.86	**0.0048**	39.17	**0.0489**	0.2428	22.63	0.2633	13.88	>0.9999	5.571	>0.9999	21.57	>0.9999	31	0.3115
Asn	**<0.0001**	47.67	**<0.0001**	21.25	**0.0233**	43.13	**0.0003**	62.71	**0.0004**	27.67	**0.0476**	0.1012	15.75	0.7656	15.13	0.7373	21.43	0.2235	24.86	0.6127	47	**0.0185**
Ile	**0.0006**	69.08	**0.0004**	31.75	0.2091	24.25	>0.9999	80.43	**0.0016**	42.5	0.2167	0.0535	43.75	0.0699	33.38	**0.0371**	6.714	>0.9999	23.14	>0.9999	30.2	0.0826
Leu	**<0.0001**	60.58	**<0.0001**	24.67	0.2073	24.5	0.1727	71.29	**0.0003**	37.5	0.0635	0.0879	32	0.0759	21.5	0.1328	5.286	>0.9999	14.43	>0.9999	22.8	0.0997
Phe	**0.0007**	41	**0.0008**	13.92	0.4929	24.75	**0.048**	53.14	**0.0008**	28.17	0.1214	0.7512	10.75	>0.9999	6.5	>0.9999	2	>0.9999	1	>0.9999	19.2	>0.9999
Trp	**0.0539**	36.83	**0.0142**	13.33	>0.9999	21	0.195	26.71	>0.9999	5.167	>0.9999	**0.0291**	12	>0.9999	14.75	>0.9999	−15.57	0.6823	−31.14	0.1187	−1.8	>0.9999
Tyr	**0.0003**	56.75	**0.0003**	31.75	0.0759	38.88	**0.0124**	63.29	**0.0004**	38.67	**0.0375**	0.2771	20	>0.9999	17.63	>0.9999	10.29	>0.9999	3.286	>0.9999	28.4	0.6478
Val	**0.0118**	26.25	**0.0013**	11.08	0.2421	13.13	0.2827	26.57	**0.0475**	10.67	0.3723	0.148	10.5	0.837	13.38	0.0637	4	>0.9999	−0.7143	>0.9999	11	0.5475
Met-SO	0.063	38	0.672	30.14	0.9448	34.75	>0.9999	116.7	**0.0204**	113.5	0.1624	0.9454	240.6	>0.9999	226.4	>0.9999	833.8	>0.9999	125	>0.9999	56.25	>0.9999
PC aa C30:0	0.0566	19.25	0.2935	7.833	>0.9999	42.38	0.1132	46	0.2131	5	>0.9999	0.5601	−5.875	>0.9999	−5.375	>0.9999	6	>0.9999	−16.71	>0.9999	−11.4	>0.9999
PC aa C38:6	0.0657	13.92	0.5686	9.75	>0.9999	4	>0.9999	17.86	>0.9999	−18.5	0.4409	**0.0243**	−2.75	>0.9999	5.75	>0.9999	−17	>0.9999	−34.86	0.1757	−28	0.4232
PC aa C40:1	0.5102	6.583	>0.9999	6.167	>0.9999	8.25	0.8057	8.143	>0.9999	0	>0.9999	**0.0234**	8.375	>0.9999	13.13	>0.9999	−20	0.5132	−21.57	0.3441	−16.4	0.7246
PC ae C42:0	0.5951	7.833	0.4055	6.667	>0.9999	7.75	0.8341	9.286	>0.9999	-1	>0.9999	0.5154	4.625	>0.9999	9.25	>0.9999	8.429	>0.9999	−11.57	>0.9999	−2.8	>0.9999
PC ae C42:4	0.3738	11.25	0.2456	4.25	>0.9999	18.38	>0.9999	19.71	0.6419	4.667	>0.9999	**0.0052**	−6.5	>0.9999	0.875	>0.9999	−15.43	0.3501	−34.43	**0.0038**	−20.2	0.3293
PC ae C44:3	0.7392	6.5	>0.9999	4.917	>0.9999	22.75	>0.9999	20.29	>0.9999	7.5	>0.9999	0.1296	12.25	>0.9999	24.75	0.5477	19.29	>0.9999	−11	>0.9999	−9	>0.9999
PC ae C44:6	0.5176	8.167	>0.9999	1.25	>0.9999	13	>0.9999	20.29	0.7778	2.833	>0.9999	**0.0166**	−10.75	>0.9999	−3.5	>0.9999	−13.57	0.8398	−32.57	**0.0074**	−22.2	0.1035
SM C16:0	0.0507	12.25	>0.9999	7.25	>0.9999	−3.75	0.5932	0.2857	0.9647	−14.33	0.2328	**0.0066**	−4.75	>0.9999	1.75	>0.9999	−11.57	0.4553	−24.29	**0.0415**	−20.8	0.0531
SM C20:2	0.3264	16.17	>0.9999	10	>0.9999	−7.875	>0.9999	6	>0.9999	−11.33	>0.9999	**0.0014**	0	>0.9999	7.875	>0.9999	−16.14	0.0913	−24.86	**0.0344**	−25.2	**0.0148**
SM C24:1	0.1562	12.75	0.5076	8.25	>0.9999	−5.5	>0.9999	0.1429	>0.9999	−11.67	>0.9999	0.0739	−7.5	>0.9999	2.5	>0.9999	−5.143	>0.9999	−19.29	0.275	−17.2	0.1544
SM C26:1	0.0796	8.917	0.9514	6	>0.9999	−4.75	>0.9999	−4.714	>0.9999	−16.67	0.4224	0.0986	−6	>0.9999	8	>0.9999	−7.286	>0.9999	−22.14	0.3339	−19.6	0.7613

NOTE: Statistical tests carried out are Kruskal–Wallis test for all time points and Dunn's multiple comparison tests for individual time points (*P* values <0.05 are bold). Mean values are percentage increase or decrease relative to time 0.

metabolic responses measured by FDG-PET confirmed the negative predictive value of FDG-PET for MEK inhibition (10). In this context, it is notable that we observe an increase in branched chain amino acids in nonresponders and following treatment with pictilisib which is consistent with the insulin-resistant phenotype (16). In addition, our previous studies showed a decrease in glycerophosphocholine in PI3K-activated tumors and an increase following PI3K inhibition with pictilisib (16). The fact that low levels of these phospholipids are predictive of resistance to the MEK inhibitor is consistent with the PI3K-activated metabotype. It has been shown that *de novo* PI3K activation is associated with resistance to MEK inhibitors (21), which is consistent with our metabolic findings. PI3K activation is also known to be induced as a result of MEK inhibition, but our metabolic response to doses of drug inhibiting the MAPK pathway does not recapitulate that observed upon PI3K activation whatever the therapeutic outcome. Studies aiming at the prediction of sensitivity to MEK inhibition by gene expression profiling have also shown compensatory signaling through RAS effectors other than PI3K (22). Tumors often harbor genetic abnormalities in both PI3K and MAPK pathways as observed in WM266.4 (although they are known to be driven primarily by MAPK). In addition, PI3K pathway abnormalities in the patients enrolled in the clinical study have not been determined, and melanomas have a high mutational load in addition to the known PI3K and MAPK drivers (23–25). Our exo-metabolomic data in sensitive human tumor xenograft models and clinical responders are in agreement with cellular metabolomic studies by NMR reporting decreased glycerophosphocholine levels which were associated with lowered expression of choline-kinase α following MEK inhibition (26). Increased levels of phosphatidylcholines, delivered by nanoparticles, in the cellular plasma membrane are able to activate EGFR, which is one of the major mechanisms of resistance to MEK inhibition suggesting effectors for these molecules upstream and downstream of MAPK (23, 27, 28). Similarly, previous studies established that activated sphingomyelinase leads to ceramide-mediated activation of MAPK (29). In our study, we show a decrease in sphingomyelins following MEK inhibition, suggesting complex regulation of sphingomyelins on the MAPK network.

We and others have demonstrated that levels of plasma metabolites vary throughout the day (12, 13). Reassuringly, we have demonstrated that the variations observed in the biomarker metabolites following treatment with the MEK inhibitor exceed time-of-day variations both in patients and healthy volunteers. We found that over 70% (15 of 21) of the metabolites identified preclinically translate to the clinical setting, and we also found additional metabolites that could be associated with responses using the clinical data alone. The metabolomic profiling of plasma (as opposed to tumor tissue) circumvents significant limitations of many current standard biomarkers (for example, lack of stability of phospho signals) and importantly is readily amenable to repeated sampling. In addition, the use of a mass spectrometry–based platform crucially allows for up-scaling and implementation in large studies. We emphasize, however, that this is a retrospective study with a limited sample size, and hence cannot be regarded as definitive at this time. Further investigations in an independent cohort are needed. This is challenging given the fact that MEK inhibitors are now administered in combination in the clinical setting. Although the mechanistic links between MAPK

Downloaded from mct.aacrjournals.org on November 30, 2020. © 2017 American Association for Cancer Research.

Published OnlineFirst June 21, 2017; DOI: 10.1158/1535-7163.MCT-16-0881

Table 3. Relationship between baseline candidate biomarker levels with objective response and presence of tumor *BRAF* mutation (*P* values <0.05 are bolds)

	Mann–Whitney test	Patient comparison		ROC analysis PD vs. PR			Mann–Whitney test	+/− BRAF mutation	
	P value	Median of PD (μM)	Median of PR (μM)	AUC	95% confidence interval	*P* value	*P* value	Median of mutated (μM)	Median of non mutated (μM)
Metabolites									
C3	0.6239	0.2585, $n = 12$	0.2396, $n = 8$	0.5729	0.3121–0.8337	0.5892	0.3114	0.2737, $n = 7$	0.2520, $n = 13$
Arg	**0.0096**	64.51, $n = 12$	87.93, $n = 8$	**0.8438**	0.6646–1.023	0.0109	>0.9999	71.06, $n = 7$	72.84, $n = 13$
Asn	0.6784	43.60, $n = 12$	43.44, $n = 8$	0.5625	0.3029–0.8221	0.6434	0.1827	44.92, $n = 7$	41.54, $n = 13$
Ile	0.5714	59.99, $n = 12$	55.37, $n = 8$	0.5833	0.3146–0.8521	0.5371	0.3114	59.88, $n = 7$	50.85, $n = 13$
Leu	0.5208	107.6, $n = 12$	101.5, $n = 8$	0.5938	0.3186–0.8689	0.4875	0.2414	102.6, $n = 7$	97.70, $n = 13$
Phe	0.0979	60.29, $n = 12$	67.46, $n = 8$	0.7292	0.5073–0.9510	0.0896	**0.0145**	75.23, $n = 7$	58.57, $n = 13$
Trp	0.238	51.96, $n = 12$	61.09, $n = 8$	0.6667	0.4182–0.9151	0.217	0.588	61.58, $n = 7$	56.64, $n = 13$
Tyr	**0.0314**	51.91, $n = 12$	66.46, $n = 8$	**0.7917**	0.5862–0.9972	0.0308	0.5356	66.20, $n = 7$	54.96, $n = 13$
Val	>0.9999	189.0, $n = 12$	178.6, $n = 8$	0.5	0.2272–0.7728	1	0.6992	185.7, $n = 7$	187.2, $n = 13$
Met-SO	0.3829	0.5386, $n = 7$	0.2994, $n = 7$	0.6531	0.3293–0.9768	0.3379	0.1469	0.2836, $n = 5$	0.5988, $n = 9$
PC aa C30:0	0.1349	2.829, $n = 12$	3.952, $n = 8$	0.7083	0.4611–0.9556	0.1228	0.7573	3.799, $n = 7$	2.895, $n = 13$
PC aa C38:6	**0.0055**	58.20, $n = 12$	115.5, $n = 8$	**0.8646**	0.6647–1.065	0.0069	0.588	100.2, $n = 7$	65.83, $n = 13$
PC aa C40:1	**0.0159**	0.3345, $n = 12$	0.4752, $n = 8$	**0.8229**	0.6194–1.026	0.0168	0.9385	0.3673, $n = 7$	0.3495, $n = 13$
PC ae C42:0	**0.0124**	0.4863, $n = 12$	0.7681, $n = 8$	**0.8333**	0.6543–1.012	0.0136	0.1146	0.7605, $n = 7$	0.5126, $n = 13$
PC ae C42:4	0.1569	0.6470, $n = 12$	0.7494, $n = 8$	0.6979	0.4640–0.9318	0.1427	0.7573	0.6656, $n = 7$	0.7221, $n = 13$
PC ae C44:3	**0.0096**	0.1298, $n = 12$	0.1833, $n = 8$	**0.8438**	0.6645–1.023	0.0109	0.1574	0.1776, $n = 7$	0.1391, $n = 13$
PC ae C44:6	0.1349	0.7642, $n = 12$	1.056, $n = 8$	0.7083	0.4555–0.9611	0.1228	0.2749	0.6329, $n = 7$	0.8804, $n = 13$
SM C16:0	0.1349	185.9, $n = 12$	203.0, $n = 8$	0.7083	0.4779–0.9388	0.1228	0.1348	197.7, $n = 7$	190.1, $n = 13$
SM C20:2	**0.0201**	0.7086, $n = 12$	1.007, $n = 8$	**0.8125**	0.6207–1.004	0.0206	**0.0085**	0.9905, $n = 7$	0.7045, $n = 13$
SM C24:1	0.1569	212.1, $n = 12$	239.0, $n = 8$	0.6979	0.4586–0.9372	0.1427	0.2106	234.1, $n = 7$	216.7, $n = 13$
SM C26:1	0.2083	0.7365, $n = 12$	0.8440, $n = 8$	0.6771	0.4319–0.9223	0.1897	**0.0111**	0.8771, $n = 7$	0.7203, $n = 13$

pathway modulation and the panel of plasma metabolite biomarkers are currently poorly understood, we anticipate that our novel findings may be helpful in guiding future investigations including those of MEK inhibitor resistance.

In summary, using LC-MS metabolomics, we showed that plasma metabolite markers of MEK inhibition can be identified in mice bearing human melanoma xenografts. In patients with advanced melanoma treated with RO4987655, the pretreatment levels of seven candidate plasma metabolite biomarkers identified in the preclinical screen were statistically significantly able to retrospectively predict objective responses to RO4987655. Our current findings and those we reported previously (10) provide a rational study design for the determination of metabolomic signatures of drug sensitivity/activity and resistance which is directly translatable to the identification of preclinical and clinical metabolomic biomarkers for other new classes of drug. Thus, metabolomics analysis can be added to the technical approaches to support the use of The Pharmacological Audit Trail for biomarker-led decision making in cancer therapeutics (30).

Disclosure of Potential Conflicts of Interest

V.L. Revell is scientific consultant at Lumie Ltd. J.S. de Bono is a consultant/advisory board member for AstraZeneca, Genentech/Roche, GSK, Merck, and Pfizer. No potential conflicts of interest were disclosed by the other authors.

Authors' Contributions

Conception and design: J.E. Ang, A. Pal, A.T. Henley, M. Venturi, J.S. de Bono, S.B. Kaye, U. Banerji, F.I. Raynaud

Development of methodology: J.E. Ang, A. Pal, Y.J. Asad, F.I. Raynaud

Acquisition of data (provided animals, acquired and managed patients, provided facilities, etc.): J.E. Ang, A. Pal, Y.J. Asad, A.T. Henley, M. Valenti, G. Box, A. de haven Brandon, V.L. Revell, J.S. de Bono, S.B. Kaye

Analysis and interpretation of data (e.g., statistical analysis, biostatistics, computational analysis): J.E. Ang, A. Pal, Y.J. Asad, V. Meresse, J.S. de Bono, P. Workman, F.I. Raynaud

Writing, review, and/or revision of the manuscript: J.E. Ang, A. Pal, Y.J. Asad, M. Venturi, V. Meresse, J.S. de Bono, S.B. Kaye, P. Workman, U. Banerji, F.I. Raynaud

Administrative, technical, or material support (i.e., reporting or organizing data, constructing databases): J.E. Ang, A. Pal, G. Box, P. Workman

Study supervision: M. Venturi, J.S. de Bono, F.I. Raynaud

Other (designed protocol and provided samples for time of day study): D.J. Skene

Acknowledgments

The authors would like to thank Chugai Pharmaceutical Co., Ltd. for providing RO4897655 to perform therapy experiment, Sharon Gowen for her MSD technical support, and Vladimir Kirkin for supporting *in vivo* therapy experiments.

Grant Support

F.I. Raynaud, P. Workman, S.A. Eccles, A. de haven Brandon, G. Box, M. Venturi, A.T. Henley, Y.J. Asad, and A. Pal are supported by a Cancer Research UK programme grant (C309/A11566) at the Cancer Research UK Cancer Therapeutics Unit. P. Workman is a Cancer Research UK Life Fellow (C309/A8992). J.E. Ang was supported by a Wellcome Trust PhD studentship grant (090952/Z/09/Z) as part of the Wellcome Trust PhD programme in mechanism-based drug discovery research project at The Institute of Cancer Research which is directed by P. Workman. The phase I clinical trial was supported by Roche, the Drug Development Unit, the Royal Marsden NHS Foundation Trust, and The Institute of Cancer Research. Support was also provided by the Experimental Cancer Medicine Centre grant to The Institute of Cancer Research and from the National Health Service to the National Institute for Health Research Biomedical Research Centre at the Institute of Cancer Research and the Royal Marsden Hospital.

The costs of publication of this article were defrayed in part by the payment of page charges. This article must therefore be hereby marked *advertisement* in accordance with 18 U.S.C. Section 1734 solely to indicate this fact.

Received December 19, 2016; revised May 31, 2017; accepted June 6, 2017; published OnlineFirst June 21, 2017.

Downloaded from mct.aacrjournals.org on November 30, 2020. © 2017 American Association for Cancer Research.

Published OnlineFirst June 21, 2017; DOI: 10.1158/1535-7163.MCT-16-0881

References

1. Wellbrock C, Karasarides M, Marais R. The RAF proteins take centre stage. Nat Rev Mol Cell Biol 2004;5:875–85.
2. Bos JL.ras oncogenes in human cancer: a review. Cancer Res 1989; 49:4682–9.
3. Roberts PJ, Der CJ. Targeting the Raf-MEK-ERK mitogen-activated protein kinase cascade for the treatment of cancer. Oncogene 2007;26:3291–310.
4. Flaherty KT, McArthur G. BRAF, a target in melanoma: implications for solid tumor drug development. Cancer 2010;116:4902–13.
5. Davies H, Bignell GR, Cox C, Stephens P, Edkins S, Clegg S, et al. Mutations of the BRAF gene in human cancer. Nature 2002;417:949–54.
6. Cantwell-Dorris ER, O'Leary JJ, Sheils OM. BRAFV600E: implications for carcinogenesis and molecular therapy. Mol Cancer Thera 2011;10:385–94.
7. Samatar AA, Poulikakos PI. Targeting RAS-ERK signalling in cancer: promises and challenges. Nat Rev Drug Discov 2014;13:928–42.
8. Richman J, Martin-Liberal J, Diem S, Larkin J. BRAF and MEK inhibition for the treatment of advanced BRAF mutant melanoma. Expert Opinion Pharmacother 2015;16:1285–97.
9. Isshiki Y, Kohchi Y, Iikura H, Matsubara Y, Asoh K, Murata T, et al. Design and synthesis of novel allosteric MEK inhibitor CH4987655 as an orally available anticancer agent. Bioorganic Med Chem Lett 2011;21:1795–801.
10. Falchook GS, Lewis KD, Infante JR, Gordon MS, Vogelzang NJ, DeMarini DJ, et al. Activity of the oral MEK inhibitor trametinib in patients with advanced melanoma: a phase 1 dose-escalation trial. Lancet Oncol 2012;13:782–9.
11. Ang JE, Pandher R, Ang JC, Asad YJ, Henley AT, Valenti M, et al. Plasma metabolomic changes following pi3k inhibition as pharmacodynamic biomarkers: preclinical discovery to phase I trial evaluation. Mol Cancer Ther 2016;15:1412–24.
12. Zimmer L, Barlesi F, Martinez-Garcia M, Dieras V, Schellens JH, Spano JP, et al. Phase I expansion and pharmacodynamic study of the oral MEK inhibitor RO4987655 (CH4987655) in selected patients with advanced cancer with RAS-RAF mutations. Clin Cancer Res 2014;20:4251–61.
13. Ang JE, Revell V, Mann A, Mantele S, Otway DT, Johnston JD, et al. Identification of human plasma metabolites exhibiting time-of-day variation using an untargeted liquid chromatography-mass spectrometry metabolomic approach. Chronobiol Int 2012;29:868–81.
14. Davies SK, Ang JE, Revell VL, Holmes B, Mann A, Robertson FP, et al. Effect of sleep deprivation on the human metabolome. Proc Nat Acad Sci USA 2014;111:10761–6.
15. Sarker D, Ang JE, Baird R, Kristeleit R, Shah K, Moreno V, et al. First-in-human phase I study of pictilisib (GDC-0941), a potent pan-class I phosphatidylinositol-3-kinase (PI3K) inhibitor, in patients with advanced solid tumors. Clin Cancer Res 2015;21:77–86.
16. Ang JE, Pandher R, Ang JC, Asad YJ, Henley A, Valenti M, et al. Plasma metabolomic changes following PI3K inhibition as pharmacodynamic biomarkers: preclinical discovery to phase I trial evaluation. Mol Cancer Thera 2016;15:1412–24.
17. Workman P, Aboagye EO, Balkwill F, Balmain A, Bruder G, Chaplin DJ, et al. Guidelines for the welfare and use of animals in cancer research. Br J Cancer 2010;102:1555–77.
18. Svensson PA, Olson FJ, Hagg DA, Ryndel M, Wiklund O, Karlstrom L, et al. Urokinase-type plasminogen activator receptor is associated with macrophages and plaque rupture in symptomatic carotid atherosclerosis. Int J Mol Med 2008;22:459–64.
19. Xia J, Wishart DS. Using metaboAnalyst 3.0 for comprehensive metabolomics data analysis. Curr Protoc Bioinformatics 2016;55:14.0.1–.0.91.
20. Bollag G, Hirth P, Tsai J, Zhang J, Ibrahim PN, Cho H, et al. Clinical efficacy of a RAF inhibitor needs broad target blockade in BRAF-mutant melanoma. Nature 2010;467:596–9.
21. Gopal YN, Deng W, Woodman SE, Komurov K, Ram P, Smith PD, et al. Basal and treatment-induced activation of AKT mediates resistance to cell death by AZD6244 (ARRY-142886) in BRAF-mutant human cutaneous melanoma cells. Cancer Res 2010;70:8736–47.
22. Dry JR, Pavey S, Pratilas CA, Harbron C, Runswick S, Hodgson D, et al. Transcriptional pathway signatures predict MEK addiction and response to selumetinib (AZD6244). Cancer Res 2010;70:2264–73.
23. Wellbrock C.MAPK pathway inhibition in melanoma: resistance three ways. Biochem Soc Transact 2014;42:727–32.
24. Hodis E, Watson IR, Kryukov GV, Arold ST, Imielinski M, Theurillat JP, et al. A landscape of driver mutations in melanoma. Cell 2012;150: 251–63.
25. Karachaliou N, Pilotto S, Teixido C, Viteri S, Gonzalez-Cao M, Riso A, et al. Melanoma: oncogenic drivers and the immune system. Ann Translat Med 2015;3:265.
26. Lodi A, Woods SM, Ronen SM. MR-detectable metabolic consequences of mitogen-activated protein kinase kinase (MEK) inhibition. NMR Biomed 2014;27:700–8.
27. Gandola YB, Perez SE, Irene PE, Sotelo AI, Miquet JG, Corradi GR, et al. Mitogenic effects of phosphatidylcholine nanoparticles on MCF-7 breast cancer cells. BioMed Res Int 2014;2014:687037.
28. Kim JY, Welsh EA, Fang B, Bai Y, Kinose F, Eschrich SA, et al. Phosphoproteomics reveals MAPK inhibitors enhance MET- and EGFR-driven AKT signaling in KRAS-mutant lung cancer. Mol Cancer Res 2016;14:1019–29.
29. Tseng TH, Shen CH, Huang WS, Chen CN, Liang WH, Lin TH, et al. Activation of neutral-sphingomyelinase, MAPKs, and p75 NTR-mediating caffeic acid phenethyl ester-induced apoptosis in C6 glioma cells. J Biom Sci 2014;21:61.
30. Banerji U, Workman P. Critical parameters in targeted drug development: the pharmacological audit trail. Sem Oncol 2016;43:436–45.

Downloaded from mct.aacrjournals.org on November 30, 2020. © 2017 American Association for Cancer Research.

Published OnlineFirst June 21, 2017; DOI: 10.1158/1535-7163.MCT-16-0881

AACR American Association for Cancer Research

Molecular Cancer Therapeutics

Modulation of Plasma Metabolite Biomarkers of the MAPK Pathway with MEK Inhibitor RO4987655: Pharmacodynamic and Predictive Potential in Metastatic Melanoma

Joo Ern Ang, Akos Pal, Yasmin J. Asad, et al.

Mol Cancer Ther 2017;16:2315-2323. Published OnlineFirst June 21, 2017.

Updated version	Access the most recent version of this article at: doi:10.1158/1535-7163.MCT-16-0881
Supplementary Material	Access the most recent supplemental material at: http://mct.aacrjournals.org/content/suppl/2017/06/21/1535-7163.MCT-16-0881.DC1

Cited articles	This article cites 30 articles, 9 of which you can access for free at: http://mct.aacrjournals.org/content/16/10/2315.full#ref-list-1
Citing articles	This article has been cited by 1 HighWire-hosted articles. Access the articles at: http://mct.aacrjournals.org/content/16/10/2315.full#related-urls

E-mail alerts	Sign up to receive free email-alerts related to this article or journal.
Reprints and Subscriptions	To order reprints of this article or to subscribe to the journal, contact the AACR Publications Department at pubs@aacr.org.
Permissions	To request permission to re-use all or part of this article, use this link http://mct.aacrjournals.org/content/16/10/2315. Click on "Request Permissions" which will take you to the Copyright Clearance Center's (CCC) Rightslink site.

Downloaded from mct.aacrjournals.org on November 30, 2020. © 2017 American Association for Cancer Research.